CHEMBIOCHEM

DOI: 10.1002/cbic.200500148

Synthesis of *N*-Heteroaryl Retinals and their Artificial Bacteriorhodopsins

Susana López,*[a] Virginia Rodríguez,[a] Javier Montenegro,[a] Carlos Saá,[a] Rosana Alvarez,[b] Carlos Silva López,[b] Angel R. de Lera,[b] Rosana Simón,[c] Tzvetana Lazarova,[c] and Esteve Padrós[c]

*N-Heteroaryl retinals derived from indole, 1-indolizine and 3-indolizine (**10a–c**) have been synthesized after their UV/Vis red-shifted absorption properties had been predicted by time-dependent density functional theory (TD-DFT) computations. The three new analogues form artificial pigments upon recombination with bacterioopsin: indolyl retinal **10a** undergoes fast and efficient reconstitution to form a species with a UV/Vis absorbance maximum similar to that of wild-type bacteriorhodopsin, whilst the indolizinyl retinals **10b** and **10c** also reconstitute in significant proportion to give noticeably red-shifted, although unstable, pigments. Significant changes in the pK_a values of these artificial bacteriorhodopsins are interpreted as arising from nonoptimal binding-site occupancy by the chromophore due to steric constraints.*

Introduction

Since its discovery in 1971, bacteriorhodopsin (bR), a photoreceptor pigment found in the purple membrane of *Halobacterium salinarum*, has become one of the most extensively studied proteins, due to its ready availability and its structural similarity to the vertebrate visual pigment rhodopsin, the best known member of the seven transmembrane helices G protein-coupled receptor (GPCR) superfamily.[1] The thermal and photochemical stability of the pigment have, moreover, allowed materials made of bR to find applications in bioelectronics.[2]

The light sensor in the bR protein complex is *trans*-retinal (**1**) (Scheme 1), which is covalently bound to the ε-amino group of Lys216 through a protonated Schiff base (PSB) linkage. In addition to the Schiff base, there is a positive charge located at Arg82 and counterbalancing negative charges at Asp85 and Asp212. The quadrupolar structure around the retinal chromophore is further stabilized by the presence of three water molecules. In the dark-adapted state, the pigment exhibits an absorption maximum (560 nm) that is red-shifted with respect to that of the model PSB formed from retinal (**1**) and butylamine in ethanol solution (440 nm). This energy difference (4870 cm^{-1}), termed "opsin shift",[3] is considered a reflection of the ligand–protein interactions in the binding site. Upon absorbing visible light, bR undergoes a photocycle, through a transient all-*trans* to 13-*cis* isomerization of the retinal chromophore, followed by a primary proton transfer from the Schiff base to Asp85, which in turn triggers a proton-transfer reaction; this results in the net translocation of a proton from the cytoplasm to the extracellular medium. The electrochemical potential associated with the transmembrane proton gradient is used by *H. salinarum* for ATP synthesis and bacterial survival.[4]

Approaches based on genetic engineering (site-directed mutagenesis), on chemical modification of the protein environment, and on replacement of native retinal with synthetic analogues have been used to investigate the stereoelectronic features of the bR-binding site.[5] Chromophore substitution can also provide optimized bRs that can be used as photoactive components in molecular electronic devices. In this context, chromophores that cause a red shift in the absorption of the native pigment have proved to be of particular interest, since materials made from these artificial bRs can potentially be stimulated with compact, inexpensive semiconductor lasers.[2]

Despite intense investigation in this area, only a few retinals forming red-shifted pigments have been identified (Scheme 1, Table 1). Pigments based on 13-demethyl-13-trifluoromethylretinal (**2**),[6] 14-fluororetinal (**3**),[7] guaiazulenyl derivatives (**4**, **5**)[8] or merocyanine structures (**6**[9] and **7**[10]) are the best known members of this group. Reasonable explanations for these large bathochromic shifts have been proposed: i) for guaiazulene and merocyanine derivatives, the stabilization of the corresponding PSBs by resonance to form highly stable tropyllium or cyanine ions, and ii) for fluorinated retinals, the destabilization of the ground state PSB due to the proximity of the

[a] *Dr. S. López, V. Rodríguez, J. Montenegro, Prof. Dr. C. Saá*
Departamento de Química Orgánica, Facultade de Química
Universidade de Santiago de Compostela
15782, Santiago de Compostela (Spain)
Fax: (+34) 981-595-012
E-mail: qosuslop@usc.es

[b] *Dr. R. Alvarez, C. Silva López, Prof. Dr. A. R. de Lera*
Departamento de Química Orgánica, Facultade de Química
Universidade de Vigo, 36310, Vigo (Spain)

[c] *R. Simón, Dr. T. Lazarova, Prof. Dr. E. Padrós*
Unitat de Biofísica
Departament de Bioquímica i de Biología Molecular
Facultat de Medicina, Universitat Autónoma de Barcelona
08193, Barcelona (Spain)

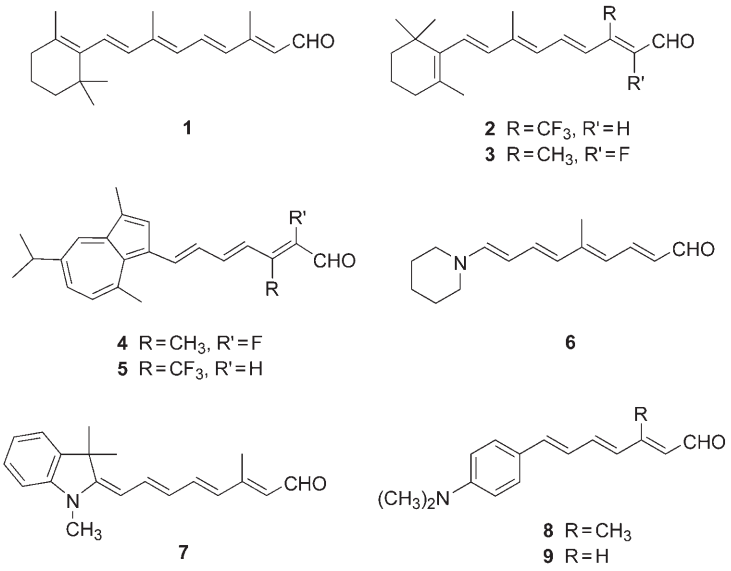

Scheme 1. Retinal (**1**) and some red-shifted analogues (**2**–**9**).

highly electron-withdrawing substituent to the positively charged nitrogen.[8–10]

In the case of the aryl polyenals,[11] in which the trimethylcyclohexenyl ring has been replaced by phenyl, naphthyl, anthryl, fluorenyl or pyrenyl systems, only derivatives containing dimethylamino groups in conjugation with the polyenic chain have provided red-shifted pigments. Sheves and co-workers have reported a group of 4-dimethylaminophenyl retinoids, with the shorter chain analogues **8** and **9** exhibiting the longest wavelengths in the series.[12]

Prompted by these precedents, we wondered what the combined effect of two of these structural modifications—the presence of an electron-donating N atom in conjugation as part of the aryl ring—might be on the absorption properties of retinals and the artificial pigments formed from them. Surprisingly, *N*-heteroaryl retinals have not been described to date, despite the fact that the conjugation of the ring heteroatom with the polyenal PSB (as isolated species in solution or as components of artificial bRs), should display contributing resonance forms reminiscent of those of the cyanine dyes. Therefore, these heteroaromatic analogues could potentially afford red-shifted pigments upon incubation with bacterioopsin.

In continuation of our studies on the chemistry and biology of synthetic retinals,[13] we report here the synthesis of three trienals containing indole (**10a**), 1-indolizine (**10b**) and 3-indolizine (**10c**) as *N*-heteroaryl rings (Scheme 2), together with the preparation of their corresponding artificial bRs.

Results and Discussion

1. UV/Vis spectra simulation—DFT calculations

Prior to synthesis, the anticipated red-shifted natures of these new retinal analogues were verified by computation of their absorption properties relative to native retinal (**1**). The use of time-dependent density functional theory (TD-DFT) for the study of electronic spectra in organic dyes has proved accurate in several recent publications.[14] A systematic benchmark of this methodology, together with semiempirical (ZINDO/S and Pariser–Parr–Pople) and experimentally determined values, has also recently been published, and showed good agreement between DFT and experimental results.[15] Moreover, TD-DFT calculations have proved reliable for modelling of the UV/Vis spectra of *trans*-retinal (**1**) and related polyenals, including some of the red-shifted analogues depicted in Scheme 1.[16]

Table 1. UV/Vis λ_{max} values for native bacteriorhodopsin and some red-shifted artificial analogues.

Compound	bR λ_{max} [nm]
1	568
2	624
3	587, 680
4	795
5	830
6	662
7	755
8	590
9	615

Table 2 lists the computed (see Experimental Section) values for the absorption maxima of analogues **10a**–**c**.[17–19] As expected, strongly red-shifted absorbance maxima were predicted for the heteroaryl retinals **10a**–**c**, especially in the case of the 3-indolizine-based analogue **10c**, which showed a shift of nearly 100 nm with respect to native retinal (**1**). For comparison, wavelengths derived from the HOMO–LUMO energy gap in the ground state were also calculated. These values are comparable to those obtained by time-dependent DFT; this indicates that the HOMOs and the LUMOs are the main orbitals compromized in the excitation process.

Table 2. Computed and experimentally determined values [nm] for the UV/Vis spectra of the new *N*-heteroaryl analogues **10a**–**c**. Time-dependent DFT vertical excitation wavelengths were calculated at the B3P86/6-31++G(d,p)//B3LYP/6-31+G(d) level; oscillator strengths are shown in parentheses. HOMO–LUMO gaps obtained at the same level of theory are also provided, together with the experimentally observed UV/Vis λ_{max} values.

Compound	TD-DFT	HOMO–LUMO gap	Experimental
10a	421 (1.26)	418	420
10b	438 (1.36)	436	460
10c	458 (1.32)	462	472

Although the absorption properties of the chromophores are known to be modulated by the protein-binding pocket, the computed red-shifted natures of **10a**–**c** appeared to represent a promising starting point for development, and so their syntheses were undertaken.

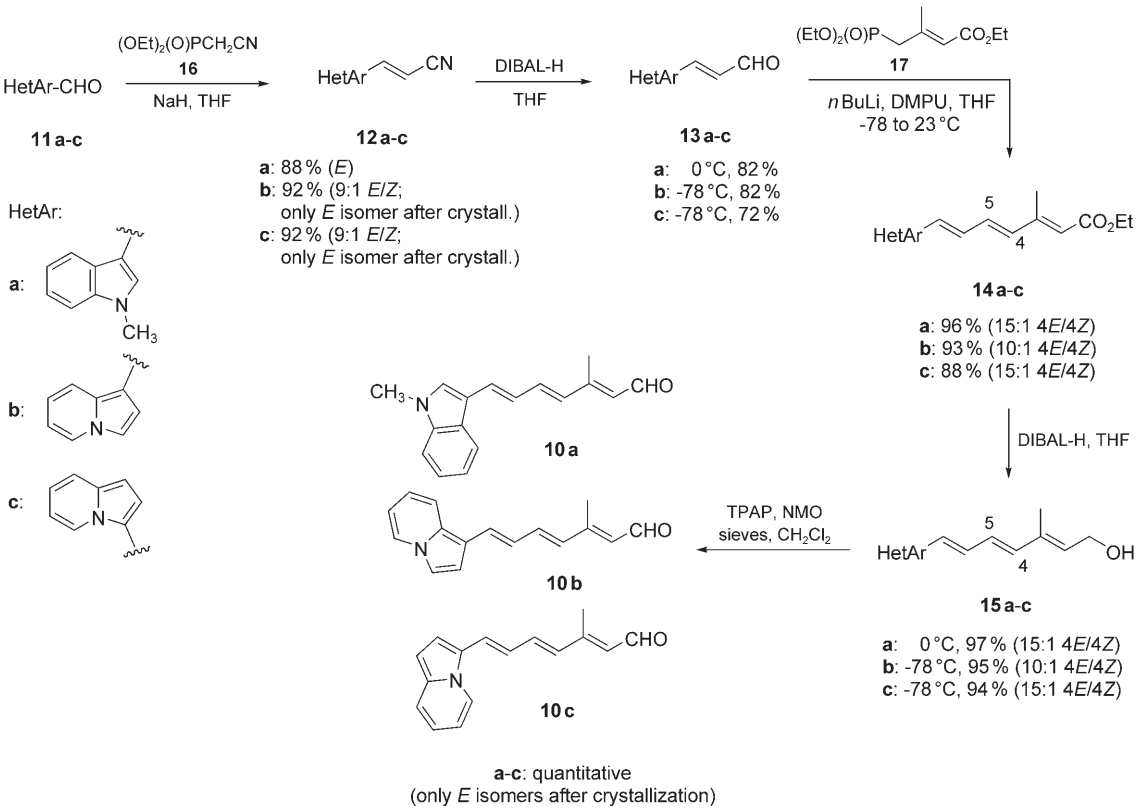

Scheme 2. Synthesis of the new *N*-heteroaryl retinals (**10a–c**).

2. Synthesis of *N*-heteroaryl retinal analogues 10a–c

The new retinals were prepared by consecutive C-2 and C-5 chain-extension reactions, starting from the corresponding heteroaromatic aldehydes,[20] by use of methods well established in retinoid synthesis (Scheme 2).[21] Compounds **11a–c** were stereoselectively converted into the vinylogous aldehydes **13a–c** in high yields through conventional Horner–Wadsworth–Emmons (HWE) reactions with diethyl (cyanomethyl)-phosphonate (**16**; NaH, THF, 23 °C) and reduction of the nitrile group with DIBAL-H. The subsequent C-5 elongation process was carried out by treating aldehydes **13a–c** with ethyl (*E*)-4-diethoxyphosphonyl-3-methylcrotonate (**17**; *n*BuLi, DMPU, THF, −78 to 23 °C) to provide esters **14a–c** in good yields and with good stereoselectivities. DIBAL-H reduction afforded the allylic alcohols **15a–c**, which were oxidized (TPAP, NMO, CH_2Cl_2, 4 Å molecular sieves) to furnish the desired retinals **10a–c** in virtually quantitative yields. Purification by column chromatography, followed by repeated crystallization (hexane/EtOAc), delivered orange solids **10a–c** as homogeneous all-*trans* isomers, as confirmed by ^1H and ^{13}C NMR spectroscopy.

The experimentally observed UV/Vis absorption maxima for the three new retinals were in good agreement (±25 nm) with the previously computed (TD-DFT) values (Table 2), thus substantiating the reliability of the calculations for the prediction of the maximum absorbances of designed chromophores. Additional bands corresponding to aryl electronic transitions were present at shorter wavelengths.

3. Preparation and photochemical properties of the Schiff bases and protonated Schiff bases

Since the chromophore in bR is bound to the protein through a protonated Schiff base, the UV/visible absorption spectra of the model Schiff bases (and their protonated forms) formed by treatment of the synthetic retinals with *n*-butylamine in methanol were recorded.[13a,22]

The values of the absorption maxima for the Schiff bases (SB-**10a–c**) and for the protonated Schiff bases (PSB-**10a–c**) of heteroaryl retinals **10a–c** in methanol are summarized in Table 3. Values for *trans*-retinal (**1**) are also included as reference.

Similarly to those of *trans*-retinal *N*-butylimine, the absorption maxima of the SBs derived from the new polyenals appear blue-shifted, with values ranging from about 30 nm for the *N*-butylimine of **10a** to about 50 nm for the SB analogue derived from **10c**.

Interestingly, protonation of these model SBs afforded species displaying UV/Vis absorption maxima (510, 574 and 610 nm, respectively) that were strongly red-shifted with respect to the model PSB made from native retinal (**1**; 440 nm). The remarkable bathochromic shifts in these *N*-heteroaryl retinal analogues were interpreted as a result of extended delocalization caused by resonance of the nitrogen electron pair with the conjugated system to form cyanine-like structures.

Table 3. *N*-heteroaryl retinals **10a–c** and their artificial bacteriorhodopsins.

Compound	Retinal[a]	SB[a]	PSB[a]	Pigments (bR)[b]	$t_{1/2}$[c]	ε_{bR}[d]	OS[e]	PRS[f]
1	381 (48000)	360	440	560	5.8	41870	4870	31.9
10a	420 (17270)	390	510	558, 582	22.3	39760	2426	27.8
10b	460 (5330)	428	574	545, 693	61.2	18800	2992	33.6
10c	472 (8160)	424	610	552, 571, 725	32.6	21690	2600	34.9

[a] UV/Vis λ_{max} [nm] values for synthetic retinals **10a–c** (extinction coefficients in parentheses), their *N*-butyl Schiff Bases (SBs) and protonated Schiff bases (PSBs) in methanol. [b] UV/Vis λ_{max} [nm] values for bR pigments **bR-10a–c** from bleached purple membranes of *Halobacterium salinarum* (strain S-9) taken in the dark-adapted state. [c] Half-lives for maximum reconstitution of the pigments [min]. [d] Extinction coefficients of the reconstituted pigments [$M^{-1}cm^{-1}$]. [e] Opsin shift, $OS = [1/\lambda_{max}PSB - 1/\lambda_{max}bR] \times 10^7$ [cm^{-1}]. [f] Percent red-shift, $PRS = [1/\lambda_{max}RETINAL - 1/\lambda_{max}bR]/[1/\lambda_{max}RETINAL] \times 10^2$ [%]. For reference, reported data for native chromophore all-*trans*-retinal (**1**) and pigment **bR-1** are also shown (Ref. [23]).

4. Preparation and properties of the artificial pigments

*4.1. Incubation of the synthetic retinals **10a–c** with bacterioopsin*:[23,24] Table 3 lists the rates of pigment formation with bacterioopsin determined from plots of the increases in absorbance at fixed wavelength—λ_{max}—against incubation time for compounds **10a–c**. All three heteroaryl retinals reacted rapidly (within minutes) with bOP although with slower rates than all-*trans*-retinal; this might be due to nonoptimal retinal–protein interaction caused by the bulk and orientation of the analogues in the binding pocket.

4.2. Absorption spectra of the pigments: Pigments derived from the indolyl retinal **10a** and the indolizinyl analogues **10b** and **10c** exhibit two or three absorption maxima at neutral pH (Figure 1). In the case of **10a** the two absorption maxima at around 558 and 582 nm overlap, resulting in a broad band centred at around 565 nm, similar to what is seen with bOP reconstituted with all-*trans* retinal (Table 3). For **10b** and **10c**, in addition to the main absorptions at 545 and 552/571 (overlapped), respectively, highly red-shifted bands (centred at 693 nm for **10b** and at 725 nm for **10c**) were also observed.

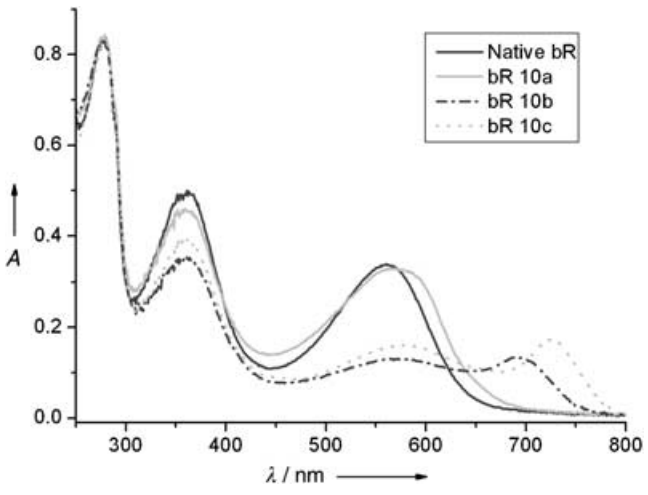

Figure 1. UV/Vis absorption spectra of dark-adapted bR pigments obtained by reconstitution of bOP with *trans*-retinal (native bR) and *N*-heteroaryl retinals (bR-**10a–c**) at neutral pH. An analogue/protein molar ratio of 1.5:1 was used for reconstitution. The band centred at about 370 nm contains contributions both from retinaloxime and from the retinal analogues present in excess.

Since titrations of the model SBs derived from **10** with 10^{-5} M HCl in MeOH (up to 6 mol equiv) each showed clear conversion of the corresponding SB maximum into a single PSB band (data not shown), it was inferred that only one protonated species was present in solution for each of the model PSBs. Therefore, the additional absorption maxima exhibited by the artificial bRs generated from **10a–c** were considered to result from specific ligand–protein interactions.

To provide further insight into the natures of the reconstituted pigments, their UV/visible spectra were recorded at several pH values (Figure 2A–C). The absorption maxima of the reconstituted pigments, unlike those of retinal-reconstituted bR, which shows a stable absorption maximum over a wide pH range, show a strong and complex dependence on pH. At acidic pH values, **10a** shows a main band at 616 nm, with a minor species absorbing around 592 nm. For **10b** and **10c**, the red-shifted species already present at neutral pH are more prominent, with maxima at about 693 and 725 nm, respectively. Minor species absorbing at about 620 and 650 are apparent for **10b** and **10c**, respectively. With an increase in pH, there is a shift to the blue for **10a**, whereas **10b** and **10c** behave differently: the most strongly red-shifted band shifts further to the red, and the originally minor band increases in intensity and shifts to the blue. At alkaline pH values, the bands are located at about 500 nm for **10a**, 515–520 nm (broad band) for **10b** and 552 nm for **10c**. Therefore, several species are present for these pigments, depending on pH.

At alkaline pH, it is significant that these maxima in all cases appear at shorter wavelengths than their counterparts for the model PSB in solution (see Table 3). These bands therefore represent unprotonated Schiff bases and can be used to obtain the apparent pK_a values of the SBs in the artificial pigments. pK_a values of about 7–8 (cf. 13.3 for native bR)[25] were determined from the plots of absorbance at λ_{max} versus pH upon titration of the alkaline form (not shown). This is in keeping with results previously found by Rousso et al. concerning substantial changes in the pK_a values of the SBs arising from structural constraints on the synthetic retinals in the binding pocket.[26]

Likewise, significant changes in the apparent pK_a of Asp85 (values between pH 5 and 7; cf. 2.6 for native bR[25c]) were obtained after plotting of the absorbance at λ_{max} of the acid form against pH for the pigments containing heteroaryl retinal analogues.

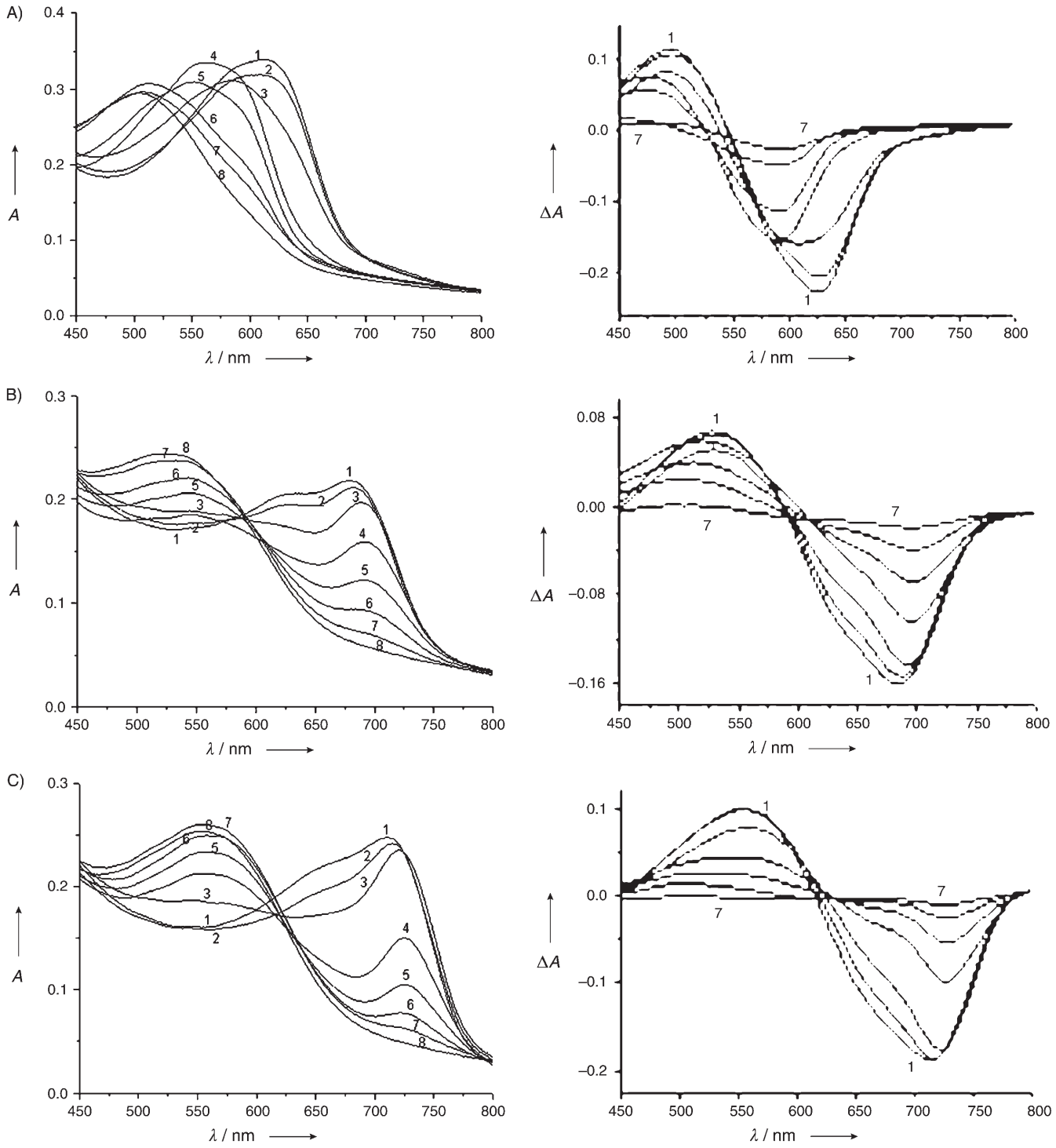

Figure 2. Left: absorption spectra of A) bR-**10a**, B) bR-**10b** and C) bR-**10c** recorded at different pH values (1: pH 3.0; 2: pH 4.0; 3: pH 5.0; 4: pH 6.5; 5: pH 7.5; 6: pH 8.5; 7: pH 9.5; 8: pH 10.5). Right: the difference spectra of the pigments at pH 10.5 (8) minus those obtained at pH values from 9.5 (7) to 3.0 (1).

Taken together, the different detected forms demonstrate the strong influence on the chromophore absorption band of the protonation states of the Schiff base, Asp85 and possibly other groups (Asp212 and Arg82 are likely candidates) capable of switching between protonated/deprotonated states. We surmise that protein conformational changes induced by the analogues alter the pK_a values of these amino acids, which revert to some extent to their normal values in a water environment.

4.3. Opsin shift (OS) and percent red shift (PRS): The opsin shift is a measure of chromophore–protein interactions in the binding site. OS values for **bR-10a**, **bR-10b** and **bR-10c** were notable (2426, 2992 and 2600 cm^{-1}, respectively Table 3), showing a significant influence of the protein environment on the absorption maxima of these pigments.

Percent red-shift (PRS) has recently been introduced as a new estimate of the extent of charge delocalization in chromo-

phores.[27] A PRS threshold of approximately 34% is strongly suggestive of the participation of a highly charge-delocalized cation. PRS values for native bR and **bR-10a–c** were 31.9%, 27.8%, 33.6% and 34.9%, respectively (Table 3). The PRS value for the pigment based on **10a** (lower than native bR) might indicate that charge delocalization through the indolyl ring is prevented in the protein binding pocket. In contrast, the high PRS values for the indolinizyl pigments **bR-10b–c** indicate their strongly delocalized natures.

4.4. Specificity and stability of the new bR analogues: Several approaches were followed to check whether the retinal analogues **10a–c** occupy the retinal binding site with involvement of a covalent bond. Additions of aldehydes **10a–c** to native bR suspensions did not result in the appearance of new absorption bands, indicating that the absorption maxima of the pigments between 500 and 725 nm correspond to true pigments and, therefore, that analogues **10a–c** do not occupy alternative unspecific binding regions of the protein.

To confirm that reconstitution gives rise to a covalent linkage between the retinal analogues and the protein, the pigment suspensions were treated with sodium borohydride under illumination at alkaline pH.[28] In all three pigments, this reaction causes the disappearance of their absorption maxima and their replacement by bands centred at about 350–360 nm, indicative of reduced SB forms. To ascertain the native binding site occupancy further, the reduced pigments were washed several times with water, all-*trans* retinal (**1**) was added, and samples were incubated for 24 h. No maxima in the 500–600 nm region were detected, as would have been the case if retinal analogues were bound to amino acids other than Lys216 of the binding pocket.

To verify the stability of the pigments, *all-trans* retinal was added to the new artificial pigments **bR-10a–c**. Slow replacement of the *N*-heteroaryl chromophores was observed for analogues **10b** and **10c**, in an exchange process requiring 48 h for completion. The indolyl analogue **10a**, however, appears to be more stable, since it persistently exhibited the characteristic broad band of the artificial pigment even after several days of competition experiments.

As a final test of pigment stability, they were treated with hydroxylamine in the dark. Unlike native bR, which is stable for several weeks in its presence, none of the *N*-heteroaryl bR analogues was stable towards treatment with 1 M NH_2OH. Noticeable differences in relative rates of pigment bleaching were observed, however, correlating well with their relative stabilities towards displacement from the binding pocket by retinal. Thus, the pigments derived from **10b** and **10c** were hydrolyzed in less than one hour in the dark with a dilute (40 mM) NH_2OH solution, whereas about two days were required to hydrolyse the **10a** analogue completely.

These results indicate that, although each of these *N*-heteroaryl retinal analogues occupies the retinal binding pocket and forms a Schiff base with Lys216, the stabilities of the artificial pigments are reduced relative to native bR, most probably due to suboptimal orientation of their ring fragments (see structures in Scheme 2 relative to native *trans*-retinal in Scheme 1), which prevent the formation of the native compact structure of the protein through steric interactions.

Conclusion

Three new retinal analogues with indole (**10a**), 1-indolizine (**10b**) and 3-indolizine (**10c**) rings at the trienal ω-position have been designed after structural considerations supported by TD-DFT computations of their absorption properties. The synthesis of these heteroaryl trienals was based on consecutive HWE condensations and adjustment of the oxidation states of the functional groups. The three heteroaryl retinals each bind to the apoprotein bOP through a covalent linkage and, although less stable than wild-type bR, appear to occupy the same binding site as native retinal. Indolyl retinal **10a** showed the fastest and most efficient reconstitution of the series, also affording the most stable pigment, with an absorption maximum similar to that of bR. The noticeably red-shifted indolizinyl derivatives bR-**10b** and bR-**10c** are less stable, however, as shown by competition experiments with the native chromophore and by treatment with hydroxylamine in the dark.

Titration experiments of these new artificial bRs reveal alterations in the pK_a values of Asp85, the Schiff base and possibly other amino acids. These alterations can be attributed to conformational changes due to nonoptimal occupancy of the native hydrophobic pocket by the heteroaryl ring. In particular, disruption of the water-bridged interactions between the SB and its Asp85 counterion could explain the changes in the pK_a values of these artificial pigments.[26]

Experimental Section

Computational methods: The structures of *N*-heteroaromatic retinals **10a–c** (Scheme 2) were optimized by use of Density Functional Theory with the three-parameter exchange functional of Becke[17] in conjunction with the gradient-corrected correlation functional of Lee, Yang and Parr.[18] Geometry optimizations were performed with the 6-31+G(d) basis set. Optimized ground state geometries were employed throughout all the excited state calculations. Vertical excitation energies and oscillator strengths were calculated by use of the time-dependent implementation of Density Functional Theory (TD-DFT). For these single-point calculations the three-parameter exchange functional of Becke was used in combination with the nonlocal correlation expression provided by the Perdew 86 functional (P86).[19] As one of the general difficulties in the computation of excited states stems from the sparse natures of their electron densities, the more extended 6–31++G(d,p) basis set was used to compute them.

General experimental procedures: Solvents were dried by published methods and were distilled before use.[29] All other reagents were commercially available compounds of the highest purity available. Reactions were carried out under argon with magnetic stirring. Analytical thin-layer chromatography (TLC) was performed on Merck silica gel (60 F-254) plates (0.25 mm) precoated with a fluorescent indicator. Flash column chromatography was performed on silica gel (230–400 mesh; flash) from Merck. Proton and carbon NMR were recorded on Bruker WM-250 (250 or 63 MHz, respectively) or Bruker AMX-300 (300 or 75 MHz, respectively) Fourier transform spectrometers, with $CDCl_3$ as solvent. Chemical shifts (δ)

are expressed in parts per million relative to tetramethylsilane as internal reference. ^{13}C multiplicities were assigned with the aid of the DEPT pulse sequence. Infrared spectra were obtained on a Bruker IFS-66 V FTIR spectrophotometer; absorptions are recorded in wavenumbers (cm^{-1}). UV/Vis spectra were recorded on a Varian Cary 100 Bio spectrophotometer with MeOH as solvent; absorption maxima are reported in nm. Low-resolution mass spectra were taken on an HP59970-GC/MS instrument operating at 70 eV. High-resolution mass spectra were taken on a Micromass Autospec instrument. Elemental analyses were obtained on a Thermo Finnigan Flash-1112 instrument. Melting points (mp) were taken on a Köfler apparatus and are uncorrected.

Synthesis

(*E*)-3-(1-Methyl-1*H*-indol-3-yl)acrylonitrile (12a)—General Procedure for HWE reactions of aldehydes 11a–c with diethyl (cyanomethyl)phosphonate (16): NaH (0.05 g, 60% in mineral oil, 1.25 mmol) was washed three times with dry ether and suspended in dry THF (2 mL). A solution of phosphonate **16** (0.22 g, 1.25 mmol) in THF (2 mL) was added dropwise and the mixture was stirred for 1 h at room temperature. After the mixture had been cooled to 0 °C, a solution of 1-methyl-1*H*-indole-3-carbaldehyde (**11a**; 0.10 g, 0.63 mmol) in dry THF was added dropwise and the reaction mixture was warmed to room temperature over 2 h. After completion of the reaction, H_2O (3 mL) was carefully added at 0 °C. The two layers were separated and the aqueous layer was extracted with ether (3×10 mL). The combined organic layers were washed with water and brine and dried over Na_2SO_4. After evaporation of the solvents, the residue was purified by flash chromatography (SiO_2, hexane/EtOAc 70:30) and crystallized to afford **12a** (0.10 g, 88%) as a pale yellow solid (mp: 100–102 °C, hexane/EtOAc). ^1H NMR (300 MHz, $CDCl_3$): $\delta = 3.69$ (s, 3H; N–Me), 5.57 (d, $J = 16.5$ Hz, 1H), 7.15 (s, 1H), 7.2–7.3 (m, 3H), 7.38 (d, $J = 16.5$ Hz, 1H), 7.63 ppm (d, $J = 7.7$ Hz, 1H); ^{13}C NMR (75 MHz, $CDCl_3$): $\delta = 33.7$ (CH_3), 89.7 (CH), 110.7 (CH), 112.2 (C), 120.5 (CH), 120.6 (C), 122.2 (CH), 123.8 (CH), 125.8 (C), 133.5 (CH), 138.5 (C), 143.9 ppm (CH); IR (CsI): $\tilde{\nu} = 2200\ cm^{-1}$ (s, CN); UV (MeOH): $\lambda_{max} = 272$, 328 nm; MS (EI^+): *m/z* (%): 182 $[M]^+$ (100), 181 (30), 140 (18); elemental analysis calcd (%) for $C_{12}H_{10}N_2$: C 79.10, N 15.37, H 5.53; found C 79.04, N 15.22, H 5.53.

(*E*)-3-(Indolizin-1-yl)acrylonitrile (12b): Indolizine-1-carbaldehyde (**11b**;[20a] 0.40 g) was converted into nitrile **12b** (0.46 g of a 9:1 *E/Z* mixture, as shown by ^1H NMR, 92%) as described above in the General Procedure. Crystallization (hexane/EtOAc) afforded **12b** as a single *E* isomer (yellow solid, mp: 136–138 °C). ^1H NMR (250 MHz, $CDCl_3$): $\delta = 5.39$ (d, $J = 16.1$ Hz, 1H), 6.57 (t, $J = 6.8$ Hz, 1H), 6.8–6.9 (m, 2H), 7.20 (d, $J = 3.0$ Hz, 1H), 7.43 (d, $J = 9.0$ Hz, 1H), 7.52 (d, $J = 16.1$ Hz, 1H), 7.86 ppm (d, $J = 6.8$ Hz, 1H); ^{13}C NMR (75 MHz, $CDCl_3$): $\delta = 87.2$ (CH), 109.8 (C), 111.9 (CH), 112.7 (CH), 116.1 (CH), 117.1 (CH), 121.0 (C), 121.9 (CH), 126.7 (CH), 134.1 (C), 141.9 ppm (CH); IR (CsI): $\tilde{\nu} = 2200\ cm^{-1}$ (s, CN); UV (MeOH): $\lambda_{max} = 240$, 348, 370 nm; MS (EI^+): *m/z* (%): 168 $[M]^+$ (100), 167 (35), 141 (18), 114 (7); HRMS (EI^+) calcd for $C_{11}H_8N_2$: 168.0687; found 168.0685.

(*E*)-3-(Indolizin-3-yl)acrylonitrile (12c): Indolizine-3-carbaldehyde (**11c**;[20b] 0.50 g) was converted into nitrile **12c** (0.58 g of a 9:1 *E/Z* mixture as shown by ^1H NMR, 92%) as described in the General Procedure above. Crystallization (hexane/EtOAc) afforded **12c** as a single *E* isomer (yellow solid, mp: 116–118 °C). ^1H NMR (250 MHz, $CDCl_3$): $\delta = 5.55$ (d, $J = 16.1$ Hz, 1H), 6.56 (d, $J = 4.4$ Hz, 1H), 6.75 (t, $J = 6.8$ Hz, 1H), 6.91 (dd, $J = 8.7$, 6.8 Hz, 1H), 7.19 (d, $J = 4.4$ Hz, 1H), 7.44 (d, $J = 8.7$ Hz, 1H), 7.55 (d, $J = 16.1$ Hz, 1H), 8.08 ppm (d, $J = 6.8$ Hz, 1H); ^{13}C NMR (75 MHz, $CDCl_3$): $\delta = 87.1$ (CH), 103.9 (CH), 113.4 (CH), 116.8 (CH), 120.2 (CH), 120.6 (C), 121.0 (C), 121.1 (CH), 123.1 (CH), 135.4 (CH), 137.8 ppm (C); IR (CsI): $\tilde{\nu} = 2200\ cm^{-1}$ (s, CN); UV (MeOH): $\lambda_{max} = 286$, 396 nm; MS (EI^+): *m/z* (%): 168 $[M]^+$ (100), 167 (67), 142 (20), 141 (21); HRMS (EI^+) calcd for $C_{11}H_8N_2$, 168.0687; found 168.0686.

(*E*)-3-(1-Methyl-1*H*-indol-3-yl)propenal (13a)—General Procedure for reduction of nitriles and esters with DIBAL-H: DIBAL-H (1.0 M in cyclohexane, 0.90 mL, 0.90 mmol) was added to a cooled (0 °C) solution of nitrile **12a** (0.15 g, 0.82 mmol) in THF (5 mL). After the mixture had been stirred at 0 °C for 3 h, H_2O was added and the mixture was extracted with Et_2O (5×). The combined organic layers were washed with a saturated aqueous $NaHCO_3$ solution, H_2O and brine, dried (Na_2SO_4) and evaporated. Purification of the residue by flash chromatography (SiO_2, 70:30 hexane/EtOAc) afforded aldehyde **13a** (0.12 g, 82%) as a yellow solid (mp: 76–78 °C, hexane/EtOAc). ^1H NMR (300 MHz, $CDCl_3$): $\delta = 3.77$ (s, 3H; N–Me), 6.66 (dd, $J = 15.7$, 7.9 Hz, 1H), 7.2–7.3 (m, 3H), 7.37 (s, 1H), 7.51 (d, $J = 15.7$ Hz, 1H), 7.82 (d, $J = 7.8$ Hz, 1H), 9.52 ppm (d, $J = 7.9$ Hz, 1H); ^{13}C NMR (75 MHz, $CDCl_3$): $\delta = 33.8$ (CH_3), 110.6 (CH), 112.8 (C), 120.9 (CH), 122.3 (CH), 123.8 (CH), 124.5 (CH), 126.3 (C), 134.6 (CH), 138.7 (C), 146.9 (CH), 194.4 ppm (CH); IR (CsI): $\tilde{\nu} = 1600\ cm^{-1}$ (s, CHO); UV (MeOH): $\lambda_{max} = 274$, 356 nm; MS (EI^+): *m/z* (%): 185 $[M]^+$ (100), 184 (32), 156 (35), 131 (87), 115 (28); elemental analysis calcd (%) for $C_{12}H_{11}NO$: C 77.81, N 7.56, H 5.99; found C 77.83, N 7.46, H 5.99.

(*E*)-3-(Indolizin-1-yl)propenal (13b): Nitrile **12b** (1.0 g, 5.95 mmol) was reduced with DIBAL-H (1.0 M in cyclohexane, 8.9 mL, 8.9 mmol) in THF (20 mL) at −78 °C for 3 h by the General Procedure to afford aldehyde **13b** (0.84 g, 82%) as an orange solid (mp: 80–82 °C, hexane/EtOAc). ^1H NMR (250 MHz, $CDCl_3$): $\delta = 6.45$ (dd, $J = 15.3$, 8.1 Hz, 1H), 6.63 (t, $J = 6.8$ Hz, 1H), 6.9–7.0 (m, 2H), 7.27 (d, $J = 2.9$ Hz, 1H), 7.59 (d, $J = 9.0$ Hz, 1H), 7.66 (d, $J = 15.3$ Hz, 1H), 7.90 (d, $J = 6.8$ Hz, 1H), 9.53 ppm (d, $J = 8.1$ Hz, 1H); ^{13}C NMR (75 MHz, $CDCl_3$): $\delta = 110.5$ (C), 113.0 (CH), 113.6 (CH), 116.6 (CH), 117.5 (CH), 122.5 (CH), 122.8 (CH), 127.0 (CH), 135.2 (C), 145.2 (CH), 193.7 ppm (CH); IR (CsI): $\tilde{\nu} = 1656$, 1629, 1603 cm^{-1} (CHO); UV (MeOH): $\lambda_{max} = 242$, 398, 416 nm; MS (EI^+): *m/z* (%): 171 $[M]^+$ (5), 117 (100), 58 (51); HRMS (EI^+) calcd for $C_{11}H_9NO$: 171.0684; found 171.0688.

(*E*)-3-(Indolizin-3-yl)propenal (13c): Nitrile **12c** (0.72 g, 4.28 mmol) was reduced with DIBAL-H (1.0 M in cyclohexane, 6.43 mL, 6.43 mmol) in THF (20 mL) at −78 °C for 3 h by the General Procedure to afford aldehyde **13b** (0.53 g, 72%) as an orange solid (mp: 80–82 °C, hexane/EtOAc). ^1H NMR (250 MHz, $CDCl_3$): $\delta = 6.51$ (dd, $J = 15.3$, 7.8 Hz, 1H), 6.58 (d, $J = 4.5$ Hz, 1H), 6.67 (t, $J = 6.8$ Hz, 1H), 6.95 (dd, $J = 8.7$, 6.8 Hz, 1H), 7.25 (d, $J = 4.5$ Hz, 1H), 7.45 (d, $J = 8.7$ Hz, 1H), 7.62 (d, $J = 15.3$ Hz, 1H), 8.22 (d, $J = 6.8$ Hz, 1H), 9.56 ppm (d, $J = 7.8$ Hz, 1H); ^{13}C NMR (75 MHz, $CDCl_3$): $\delta = 104.7$ (CH), 113.6 (CH), 119.3 (CH), 120.2 (CH), 121.3 (CH), 121.8 (CH+C), 123.8 (CH), 137.8 (CH), 139.0 (C), 193.0 ppm (CH); IR (CsI): $\tilde{\nu} = 1656$, 1602 cm^{-1} (s, CHO); UV (MeOH): $\lambda_{max} = 296$, 430 nm; MS (EI^+): *m/z* (%): 171 $[M]^+$ (51), 142 (30), 141 (56), 117 (100); HRMS (EI^+) calcd for $C_{11}H_9NO$, 171.0684; found 171.0692.

Ethyl (2*E*,4*E*,6*E*)-3-methyl-7-(1-methyl-1*H*-indol-3-yl)hepta-2,4,6-trienoate (14a)—General procedure for HWE reactions of aldehydes 13a–c with ethyl (*E*)-4-diethoxyphosphonyl-3-methylcrotonate (17): DMPU (0.56 mL, 4.64 mmol) was added to a cooled (0 °C) solution of phosphonate **17** (0.61 g, 2.32 mmol) in THF (3 mL), followed by *n*BuLi (1.6 M in hexanes, 1.44 mL, 2.32 mmol). After stirring for 20 min, the mixture was cooled to −78 °C. A solution of aldehyde **13a** (0.28 g, 1.54 mmol) in THF (2 mL) was slowly added, and the reaction mixture was stirred at −78 °C for 3 h and

then allowed to warm up to 0 °C for 18 h. Saturated aqueous NH_4Cl solution was added and the reaction mixture was extracted with Et_2O. The combined organic extracts were washed with H_2O and brine, dried (Na_2SO_4) and concentrated. Purification of the residue by chromatography (SiO_2, 70:28:2 hexane/EtOAc/Et_3N) afforded **14a** (0.43 g, 96%) as a yellow solid in a 15:1 4*E*/4*Z* isomer ratio, as determined by ^{1}H NMR. Spectroscopic data for the major (2*E*,4*E*,6*E*) isomer: ^{1}H NMR (300 MHz, $CDCl_3$): $\delta = 1.30$ (t, $J = 7.1$ Hz, 3H), 2.37 (s, 3H), 3.79 (s, 3H; N–Me), 4.21 (q, $J = 7.1$ Hz, 2H), 5.78 (s, 1H), 6.32 (d, $J = 14.4$ Hz, 1H), 6.8–7.0 (m, 3H), 7.20 (s, 1H), 7.2–7.3 (m, 2H), 7.29 (d, $J = 15.7$ Hz, 1H), 7.90 ppm (d, $J = 7.6$ Hz, 1H); ^{13}C NMR (75 MHz, $CDCl_3$): $\delta = 14.2$ (CH_3), 14.8 (CH_3), 33.4 (CH_3), 60.0 (CH_2), 110.1 (CH), 114.4 (C), 118.0 (CH), 120.6 (CH), 120.8 (CH), 122.9 (CH), 125.2 (CH), 126.4 (C), 129.5 (CH), 129.8 (CH), 133.0 (CH), 136.9 (CH), 138.2 (C), 153.4 (C), 167.8 ppm (C); IR (CsI): $\tilde{\nu} = 1702$ cm^{-1} (CO_2Et); MS (EI$^+$): *m/z* (%): 295 $[M]^+$ (27), 222 (100), 207 (37), 144 (34); HRMS (EI$^+$) calcd for $C_{19}H_{21}NO_2$, 295.1572; found 295.1581.

Ethyl (2*E*,4*E*,6*E*)-7-(indolizin-1-yl)-3-methylhepta-2,4,6-trienoate (14b): A mixture of phosphonate **17** (0.60 g, 2.19 mmol) and DMPU (0.53 mL, 4.39 mmol) in THF (3 mL) was treated with *n*BuLi (1.6 M in hexanes, 1.37 mL, 2.19 mmol) as described in the above General Procedure, followed by a solution of aldehyde **13b** (0.25 g, 1.46 mmol) in THF (2 mL), to afford **14b** (0.38 g, 93%) as an orange solid in a 10:1 4*E*/4*Z* isomer ratio as determined by ^{1}H NMR. Spectroscopic data for the major (2*E*,4*E*,6*E*) isomer: ^{1}H NMR (250 MHz, $CDCl_3$): $\delta = 1.18$ (t, $J = 7.1$ Hz, 3H), 2.27 (s, 3H), 4.07 (q, $J = 7.1$ Hz, 2H), 5.64 (s, 1H), 6.15 (d, $J = 15.0$ Hz, 1H), 6.35 (t, $J = 6.7$ Hz, 1H), 6.55 (dd, $J = 15.0$, 10.7 Hz, 1H), 6.63 (dd, $J = 9.0$, 6.7 Hz, 1H), 6.72 (dd, $J = 15.0$, 10.7 Hz, 1H), 6.85 (d, $J = 15.0$ Hz, 1H), 6.85 (d, $J = 2.6$ Hz, 1H), 7.10 (d, $J = 2.6$ Hz, 1H), 7.37 (d, $J = 9.0$ Hz, 1H), 7.69 ppm (d, $J = 6.7$ Hz, 1H); ^{13}C NMR (75 MHz, $CDCl_3$): $\delta = 14.2$ (CH_3), 14.8 (CH_3), 59.9 (CH_2), 111.4 (CH), 111.6 (CH), 112.4 (C), 114.9 (CH), 117.5 (CH), 117.7 (CH), 119.3 (CH), 123.5 (CH), 126.3 (CH), 128.3 (CH), 132.2 (CH+C), 136.8 (CH), 153.7 (C), 167.8 ppm (C); IR (CsI): $\tilde{\nu} = 1702$ cm^{-1} (s, CO_2Et); MS (EI$^+$): *m/z* (%): 281 $[M]^+$ (20), 208 (100), 193 (29), 130 (52); HRMS (EI$^+$) calcd for $C_{18}H_{19}NO_2$, 281.1416; found 281.1425.

Ethyl (2*E*,4*E*,6*E*)-7-(indolizin-3-yl)-3-methylhepta-2,4,6-trienoate (14c): A mixture of phosphonate **17** (0.60 g, 2.19 mmol) and DMPU (0.53 mL, 4.39 mmol) in THF (3 mL) was treated with *n*BuLi (1.6 M in hexanes, 1.37 mL, 2.19 mmol) as described in the above General Procedure, followed by a solution of aldehyde **13c** (0.25 g, 1.46 mmol) in THF (20 mL), to afford **14c** (0.36 g, 88%) as an orange solid in a 15:1 4*E*/4*Z* isomer ratio as determined by ^{1}H NMR. Spectroscopic data for the major (2*E*,4*E*,6*E*) isomer: ^{1}H NMR (250 MHz, $CDCl_3$): $\delta = 1.29$ (t, $J = 7.1$ Hz, 3H), 2.36 (s, 3H), 4.17 (q, $J = 7.1$ Hz, 2H), 5.77 (s, 1H), 6.31 (d, $J = 14.2$ Hz, 1H), 6.50 (d, $J = 4.1$ Hz, 1H), 6.59 (t, $J = 6.8$ Hz, 1H), 6.75 (dd, $J = 8.7$, 6.8 Hz, 1H), 6.7–6.8 (m, 2H), 6.90 (d, $J = 14.4$ Hz, 1H), 7.08 (d, $J = 4.1$ Hz, 1H), 7.37 (d, $J = 8.7$ Hz, 1H), 8.00 ppm (d, $J = 6.8$ Hz, 1H); ^{13}C NMR (63 MHz, $CDCl_3$): $\delta = 14.2$ (CH_3), 14.8 (CH_3), 60.0 (CH_2), 102.4 (CH), 112.1 (CH), 113.7 (CH), 118.3 (CH), 118.4 (CH), 120.1 (CH), 122.3 (CH), 122.6 (CH), 123.9 (C), 124.6 (CH), 133.9 (CH), 135.5 (C), 136.0 (CH), 153.1 (C), 167.7 ppm (C); IR (CsI): $\tilde{\nu} = 1703$ cm^{-1} (CO_2Et); MS (EI$^+$): *m/z* (%): 281 $[M]^+$ (30), 208 (100), 193 (25), 154 (11), 130 (23); HRMS (EI$^+$) calcd for $C_{18}H_{19}NO_2$: 281.1416; found 281.1413.

(2*E*,4*E*,6*E*)-3-Methyl-7-(1-methyl-1*H*-indol-3-yl)hepta-2,4,6-trien-1-ol (15a): A solution of ethyl ester **14a** (0.26 g, 0.88 mmol) in THF (5 mL) was treated with DIBAL-H (1.0 M in cyclohexane, 2.20 mL, 2.20 mmol) at 0 °C for 3 h as described in the General Procedure for **13a**, to afford aldehyde **15a** (0.21 g, 97%) as a yellow solid in the same isomer ratio (4*E*/4*Z* 15:1) as the starting compound. Spectroscopic data for the major (2*E*,4*E*,6*E*) isomer: ^{1}H NMR (300 MHz, $CDCl_3$): $\delta = 1.89$ (s, 3H), 3.74 (s, 3H), 4.32 (d, $J = 7.1$ Hz, 2H), 5.69 (t, $J = 7.1$ Hz, 1H), 6.32 (d, $J = 15.6$ Hz, 1H), 6.47 (dd, $J = 14.9$, 8.6 Hz, 1H), 6.7–6.9 (m, 2H), 7.13 (s, 1H), 7.2–7.3 (m, 3H), 7.90 ppm (d, $J = 8.0$ Hz, 1H); ^{13}C NMR (75 MHz, $CDCl_3$): $\delta = 12.6$ (CH_3), 32.8 (CH_3), 59.4 (CH_2), 109.4 (CH), 114.0 (C), 119.9 (CH), 120.0 (CH), 122.1 (CH), 125.4 (CH), 125.5 (CH), 125.9 (C), 128.1 (CH), 128.8 (CH), 130.2 (CH), 133.7 (CH), 136.7 (C), 137.5 ppm (C); IR (CsI): $\tilde{\nu} = 3415$ cm^{-1} (br, OH); UV (MeOH): $\lambda_{max} = 240$, 344 nm; MS (EI$^+$): *m/z* (%): 253 $[M]^+$ (40), 222 (91), 167 (257), 144 (100); HRMS (EI$^+$) calcd for $C_{17}H_{19}NO$: 253.1467; found 253.1461.

(2*E*,4*E*,6*E*)-7-(Indolizin-1-yl)-3-methylhepta-2,4,6-trien-1-ol (15b): A solution of ethyl ester **14b** (0.22 g, 0.80 mmol) in THF (5 mL) was treated with DIBAL-H (1.0 M in cyclohexane, 2.0 mL, 2.0 mmol) at −78 °C for 3 h as described in the above General Procedure to afford aldehyde **15b** (0.18 g, 95%) as a yellow solid in the same isomer ratio (4*E*/4*Z* 10:1) as the starting compound. Spectroscopic data for the major (2*E*,4*E*,6*E*) isomer: ^{1}H NMR (300 MHz, $CDCl_3$): $\delta =$ 1.87 (s, 3H), 4.30 (d, $J = 7.0$ Hz, 2H), 5.66 (t, $J = 7.0$ Hz, 1H), 6.28 (d, $J = 15.1$ Hz, 1H), 6.43 (t, $J = 6.7$ Hz, 1H), 6.55 (dd, $J = 15.1$, 10.7 Hz, 1H), 6.65 (dd, $J = 15.1$, 10.7 Hz, 1H), 6.71 (dd, $J = 9.0$, 6.7 Hz, 1H), 6.84 (d, $J = 15.1$ Hz, 1H), 6.95 (d, $J = 2.8$ Hz, 1H), 7.23 (d, $J = 2.8$ Hz, 1H), 7.47 (d, $J = 9.0$ Hz, 1H), 7.82 ppm (d, $J = 6.7$ Hz, 1H); ^{13}C NMR (75 MHz, $CDCl_3$): $\delta = 12.6$ (CH_3), 59.5 (CH_2), 110.6 (CH), 110.8 (CH), 112.2 (C), 113.9 (CH), 117.4 (CH), 118.0 (CH), 124.1 (CH), 124.4 (CH), 125.7 (CH), 128.5 (CH), 130.3 (CH), 131.0 (C), 133.2 (CH), 137.2 ppm (C); IR (CsI): $\tilde{\nu} = 3429$ cm^{-1} (br, OH); UV (MeOH): $\lambda_{max} = 256$, 370 nm; MS (EI$^+$): *m/z* (%): 239 $[M]^+$ (77), 208 (100), 193 (25), 154 (15), 130 (28); HRMS (EI$^+$) calcd for $C_{16}H_{17}NO$, 239.1310; found 239.1314.

(2*E*,4*E*,6*E*)-7-(Indolizin-3-yl)-3-methylhepta-2,4,6-trien-1-ol (15c): A solution of ethyl ester **14c** (0.20 g, 0.70 mmol) in THF (5 mL) was treated with DIBAL-H (1.0 M in cyclohexane, 1.75 mL, 1.75 mmol) at −78 °C for 3 h as described in the above General Procedure to afford aldehyde **15b** (0.16 g, 94%) as a yellow solid in the same isomer ratio (4*E*/4*Z* 15:1) as the starting compound. Spectroscopic data for the major (2*E*,4*E*,6*E*) isomer: ^{1}H NMR (250 MHz, $CDCl_3$): $\delta =$ 1.87 (s, 3H), 4.31 (d, $J = 6.5$ Hz, 2H), 5.70 (t, $J = 6.5$ Hz, 1H), 6.33 (d, $J = 15.1$ Hz, 1H), 6.47 (d, $J = 4.0$ Hz, 1H), 6.56 (t, $J = 6.8$ Hz, 1H), 6.5–6.8 (m, 2H), 6.67 (dd, $J = 8.7$, 6.8 Hz, 1H), 6.77 (d, $J = 13.7$ Hz, 1H), 7.02 (d, $J = 4.0$ Hz, 1H), 7.35 (d, $J = 8.7$ Hz, 1H), 7.98 ppm (d, $J =$ 6.8 Hz, 1H); ^{13}C NMR (63 MHz, $CDCl_3$): $\delta = 13.0$ (CH_3), 59.9 (CH_2), 101.7 (CH), 111.6 (CH), 112.6 (CH), 117.5 (CH), 119.3 (CH), 120.0 (CH), 122.4 (CH), 124.1 (C), 126.1 (CH), 129.9 (CH), 130.1 (CH), 134.8 (C), 135.4 (CH), 137.2 ppm (C); IR (CsI): $\tilde{\nu} = 3429$ cm^{-1} (br, OH); UV (MeOH): $\lambda_{max} = 294$, 400 nm; MS (EI$^+$): *m/z* (%): 239 $[M]^+$ (70), 208 (100), 193 (28), 168 (30), 154 (38), 130 (61); HRMS (EI$^+$) calcd for $C_{16}H_{17}NO$: 239.1310; found 239.1317.

(2*E*,4*E*,6*E*)-3-Methyl-7-(1-methyl-1*H*-indol-3-yl)hepta-2,4,6-trienal (10a)–-General Procedure for oxidation of allylic alcohols with TPAP: TPAP (7 mg, 0.02 mmol) was added in one portion to a stirred mixture of alcohol **15a** (0.10 g, 0.40 mmol), NMO (0.07 g, 0.60 mmol) and powdered molecular sieves (4 Å, 0.2 g) in CH_2Cl_2 (4 mL). After stirring for 2 h, the reaction mixture was filtered through a short pad of silica gel. The filtrate was evaporated and the residue (quantitative yield) was crystallized to afford pure all-*trans*-**10a** as an orange solid (mp: 123–125 °C, hexane/EtOAc). ^{1}H NMR (300 MHz, $CDCl_3$): $\delta = 2.34$ (s, 3H), 3.80 (s, 3H), 5.97 (d, $J =$ 8.1 Hz, 1H), 6.40 (d, $J = 14.3$ Hz, 1H), 6.9–7.0 (m, 3H), 7.23 (s, 1H), 7.2–7.3 (m, 3H), 7.89 (d, $J = 7.6$ Hz, 1H), 10.11 ppm (d, $J = 8.1$ Hz, 1H); ^{13}C NMR (75 MHz, $CDCl_3$): $\delta = 13.1$ (CH_3), 33.1 (CH_3), 109.8 (CH), 113.9 (C), 120.1 (CH), 120.6 (CH), 122.6 (CH), 124.3 (CH), 125.9 (C), 128.2 (CH), 129.9 (CH), 130.9 (CH), 131.7 (CH), 137.7 (C), 138.3 (CH),

155.2 (C), 190.8 ppm (CH); IR (CsI): $\tilde{\nu}=1650\ cm^{-1}$ (s, CHO); UV (MeOH) $\lambda_{max}=296$, 420 nm; MS (EI^+): *m/z* (%): 251 $[M]^+$ (89), 222 (96), 208 (46), 182 (56), 157 (48), 144 (100); HRMS (EI^+) calcd for $C_{17}H_{17}NO$: 251.1310; found 251.1317.

(2*E*,4*E*,6*E*)-7-(Indolizin-1-yl)-3-methylhepta-2,4,6-trienal (10b): Allylic alcohol **15b** (0.05 g, 0.21 mmol) was treated with NMO (0.04 g, 0.32 mmol), molecular sieves (4 Å, 0.10 g) and TPAP (4 mg, 0.01 mmol) in CH_2Cl_2 (2 mL) by the General Procedure, to afford, after crystallization, pure all-*trans*-**10b** as an orange solid (mp: 133–135 °C, hexane/EtOAc). ^1H NMR (250 MHz, $CDCl_3$): $\delta=2.33$ (s, 3H), 5.97 (d, $J=8.2$ Hz, 1H), 6.36 (d, $J=15.0$ Hz, 1H), 6.55 (t, $J=6.7$ Hz, 1H), 6.73 (dd, $J=15.0$, 10.9 Hz, 1H), 6.83 (dd, $J=9.0$, 6.7 Hz, 1H), 6.98 (dd, $J=15.1$, 10.9 Hz, 1H), 7.00 (d, $J=2.9$ Hz, 1H), 7.07 (d, $J=15.1$ Hz, 1H), 7.27 (d, $J=2.9$ Hz, 1H), 7.53 (d, $J=9.0$ Hz, 1H), 7.89 (d, $J=6.7$ Hz, 1H), 10.09 ppm (d, $J=8.2$ Hz, 1H); ^{13}C NMR (75 MHz, $CDCl_3$): $\delta=13.1$ (CH_3), 111.1 (CH), 111.4 (CH), 111.9 (C), 114.8 (CH), 117.2 (CH), 119.4 (CH), 122.8 (CH), 125.9 (CH), 127.8 (CH), 129.5 (CH), 130.9 (CH), 132.2 (C), 138.1 (CH), 155.3 (C), 190.7 ppm (CH); IR (CsI): $\tilde{\nu}=1665\ cm^{-1}$ (s, CHO); UV (MeOH): $\lambda_{max}=$ 240, 320, 460 nm; MS (EI^+): *m/z* (%): 237 $[M]^+$ (55), 208 (75), 193 (47), 168 (61), 143 (62), 142 (58), 130 (100); HRMS (EI^+) calcd for $C_{16}H_{15}NO$: 237.1154; found 237.1158.

(2*E*,4*E*,6*E*)-7-(Indolizin-3-yl)-3-methylhepta-2,4,6-trienal (10c): Allylic alcohol **15c** (0.05 g, 0.21 mmol) was treated with NMO (0.04 g, 0.32 mmol), molecular sieves (4 Å, 0.10 g) and TPAP (4 mg, 0.01 mmol) in CH_2Cl_2 (2 mL) by the General Procedure, to afford, after crystallization, pure all-*trans*-**10c** as an orange solid (mp: 122–124 °C, hexane/EtOAc). ^1H NMR (250 MHz, $CDCl_3$): $\delta=2.31$ (s, 3H), 5.96 (d, $J=8.2$ Hz, 1H), 6.37 (d, $J=15.1$ Hz, 1H), 6.53 (d, $J=4.3$ Hz, 1H), 6.64 (t, $J=6.9$ Hz, 1H), 6.75 (dd, $J=8.8$, 6.9 Hz, 1H), 6.77 (dd, $J=15.1$, 10.1 Hz, 1H), 6.95 (dd, $J=14.3$, 10.1 Hz, 1H), 6.99 (d, $J=14.3$ Hz, 1H), 7.12 (d, $J=4.3$ Hz, 1H), 7.39 (d, $J=8.8$ Hz, 1H), 8.04 (d, $J=6.9$ Hz, 1H), 10.09 ppm (d, $J=8.2$ Hz, 1H); ^{13}C NMR (75 MHz, $CDCl_3$): $\delta=13.4$ (CH_3), 102.9 (CH), 112.4 (CH), 114.4 (CH), 119.0 (CH), 120.1 (CH), 122.7 (CH), 123.8 (CH), 123.9 (CH+C), 128.7 (CH), 132.9 (CH), 136.0 (C), 137.8 (CH), 155.4 (C), 191.4 ppm (CH); IR (CsI): $\tilde{\nu}=1653\ cm^{-1}$ (s, CHO); UV (MeOH): $\lambda_{max}=240$, 324, 472 nm; MS (EI^+): *m/z* (%): 237 $[M]^+$ (62), 208 (74), 193 (46), 168 (79), 130 (76), 117 (61), 58 (100); HRMS (EI^+) calcd for $C_{16}H_{15}NO$: 237.1154; found 237.1156.

Preparation of the Schiff bases and protonated Schiff bases: *n*-Butylamine (0.2 mL) was added under nitrogen to a solution of the retinal analogue (1.0 mL, 5.0×10^{-3} M) in anhydrous ether. After addition of a few molecular sieves (4 Å), the mixture was kept at 4 °C under nitrogen overnight. Filtration and solvent evaporation under a stream of nitrogen and then under vacuum (pump) provided the desired Schiff base. Its protonation was effected in the UV cuvette by addition of a drop of methanolic HCl (3%) to the Schiff base (3.0 mL of a 5.0×10^{-5} M solution in methanol).

Preparation of bacterioopsin and incubation of analogues: The apoprotein bacterioopsin (bOP) was prepared by bleaching the purple membrane of *H. salinarum* by the procedure described earlier.[23] Its functionality was confirmed by its ability to regenerate bR upon addition of retinal (**1**).

Suspensions of bOP (1.0×10^{-5} M) in phosphate buffer (50 mM, pH 6.5) were incubated with the retinal analogues dissolved in ethanol. The ethanol concentration in all samples was always kept below 0.5% of the total volume. The analogue/apoprotein ratio used for pigment reconstitution was 1.5:1 (mol/mol), as determined from the values of the extinction coefficients of bOP ($90\,000\ M^{-1}cm^{-1}$ at 280 nm) and the retinal analogues. Samples were incubated at room temperature and sonicated ($2\times10''$) to improve reconstitution and to decrease protein aggregation.[24]

Acknowledgements

We thank the Ministerio de Ciencia y Tecnología (Grant BMC2003-04941), the European Regional Development Fund (Projects BQU2002-02135 and SAF2004-07131) and the Xunta de Galicia (Project PGIDT00PXI20901PR) for financial support. J.M., C.S. (FPU fellowships) and R.A. (Ramón y Cajal Contract) also thank MCYT/MEC.

Keywords: ab initio calculations · artificial bacteriorhodopsins · dyes/pigments · *N*-heteroaryl retinals · UV-visible spectra simulation

[1] For reviews on bacteriorhodopsin, rhodopsin and G protein-coupled receptors, see: a) W. Stoeckenius, R. H. Lozier, R. A. Bogomolni, *Biochim. Biophys. Acta* **1978**, *505*, 215; b) J. K. Lanyi, H. Luecke, *Curr. Opin. Struct. Biol.* **2001**, *11*, 415; c) T. P. Sakmar, *Curr. Opin. Cell Biol.* **2002**, *14*, 189; d) S. Filipek, R. E. Stenkamp, D. C. Teller, K. Palczewski, *Annu. Rev. Physiol.* **2003**, *65*, 851; e) P. S. Park, S. Filipek, J. W. Wells, K. Palczewski, *Biochemistry* **2004**, *43*, 15643; f) M. A. van der Horst, K. Hellingwerf, *Acc. Chem. Res.* **2004**, *37*, 13.

[2] a) K. J. Wise, N. B. Gillespie, J. A. Stuart, M. P. Krebs, R. R. Birge, *Trends Biotechnol.* **2002**, *20*, 387; b) N. Hampp, *Chem. Rev.* **2000**, *100*, 1755.

[3] K. Nakanishi, V. Balogh-Nair, M. Arnaboldi, K. Tsujimoto, B. Honig, *J. Am. Chem. Soc.* **1980**, *102*, 7945.

[4] a) A. Royant, K. Edman, T. Ursby, E. Pebay-Peyroula, E. M. Landau, R. Neutze, *Nature* **2000**, *406*, 645; b) H. J. Sass, G. Buldt, R. Gessenich, D. Hehn, D. Neff, R. Schlesinger, J. Berendzen, P. Ormos, *Nature* **2000**, *406*, 649; c) S. Subramaniam, R. Henderson *Nature* **2000**, *406*, 653; d) J. K. Lanyi, *J. Phys. Chem. B* **2000**, *104*, 11441; e) T. Hirai, S. Subramaniam, *FEBS Lett.* **2003**, *545*, 2; f) Y. Lee, M. *Krauss, J. Am. Chem. Soc.* **2004**, *126*, 2225.

[5] K. Nakanishi, R. Crouch, *Isr. J. Chem.* **1995**, *35*, 253.

[6] W. Gärtner, D. Oesterhelt, P. Towner, H. Hopf, L. Ernst, *J. Am. Chem. Soc.* **1981**, *103*, 7642.

[7] a) M. E. Tierno, D. Mead, A. E. Asato, R. S. H. Liu, N. Sekiya, K. Yoshihara, C. W. Chang, K. Nakanishi, R. Govindjee, T. G. Ebrey, *Biochemistry* **1990**, *29*, 5948; b) A. B. Druzhko, B. Robertson, R. Alvarez, A. R. de Lera, H. H. Weetall, *Biochim. Biophys. Acta* **1998**, *1371*, 371.

[8] a) A. E. Asato, X.-Y. Li, D. Mead, G. M. L. Patterson, R. S. H. Liu, *J. Am. Chem. Soc.* **1990**, *112*, 7398; b) J. R. Bell, R. S. Muthyala, R. W. Larsen, M. Alam, R. S. H. Liu, *J. Phys. Chem. A* **1998**, *102*, 5481.

[9] F. Derguini, C. G. Caldwell, M. G. Motto, V. Balogh-Nair, K. Nakanishi, *J. Am. Chem. Soc.* **1983**, *105*, 646.

[10] D. Hoischen, S. Steinmüller, W. Gärtner, V. Buss, H.-D. Martin, *Angew. Chem.* **1997**, *109*, 1702; *Angew. Chem. Int. Ed. Engl.* **1997**, *36*, 1630.

[11] a) A. Maeda, A. E. Asato, R. S. H. Liu, T. Yoshizawa, *Biochemistry* **1984**, *23*, 2507; b) R. S. H. Liu, E. Krogh, X.-Y. Li, D. Mead, L. U. Colmenares, J. R. Thiel, J. Ellis, D. Wong, A. E. Asato, *Photochem. Photobiol.* **1993**, *58*, 701; c) D. Ivanova, V. Kolev, T. Lazarova, E. Padrós, *Tetrahedron Lett.* **1999**, *40*, 2645; d) A. K. Singh, D. Manjula, *Photochem. Photobiol.* **2003**, *78*, 503.

[12] a) M. G. Motto, M. Sheves, K. Tsujimoto, V. Balogh-Nair, K. Nakanishi, *J. Am. Chem. Soc.* **1980**, *102*, 7947; b) M. Sheves, N. Friedman, A. Albeck, M. Ottolenghi, *Biochemistry* **1985**, *24*, 1260.

[13] a) A. R. de Lera, B. Iglesias, J. Rodríguez, R. Alvarez, S. López, X. Villanueva, E. Padrós, *J. Am. Chem. Soc.* **1995**, *117*, 8220; b) A. Francesch, R. Alvarez, S. López, A. R. de Lera, *J. Org. Chem.* **1997**, *62*, 310; c) L. Colmenares, X. I. Zou, J. Liu, A. Asato, R. S. H. Liu, A. R. de Lera, R. Alvarez, *J. Am. Chem. Soc.* **1999**, *121*, 5803; d) R. Alvarez, M. Domínguez, Y. Pazos, F. Sussman, A. R. de Lera, *Chem. Eur. J.* **2003**, *9*, 5821.

[14] a) P. Mach, J. Urban, J. Leszczynski, *Int. J. Quantum Chem.* **2002**, *87*, 265; b) M. Parac, S. Grimme, *Chem. Phys.* **2003**, *292*, 11; c) B. Durbeej, L. A.

Erikson, *Chem. Phys. Lett.* **2003**, *375*, 30; d) L. Shen, H.-Y. Zhang, H.-F. Ji, *Org. Lett.* **2005**, *7*, 243.
[15] a) J. Fabian, *Theor. Chem. Acc.* **2001**, *106*, 199; b) M. Wanko, M. Hoffmann, P. Strodel, A. Koslowski, W. Thiel, F. Neese, T. Frauenheim, M. Elstner, *J. Phys. Chem. B* **2005**, *109*, 3606.
[16] C. Silva López, O. Nieto Faza, S. López, A. R. de Lera, *J. Comput. Chem.* **2005**, in press. DOI: 10.1002/jcc.20305.
[17] a) A. D. Becke, *Phys. Rev. A* **1988**, *38*, 3098; b) A. D. Becke, *J. Chem. Phys.* **1993**, *98*, 5648.
[18] C. Lee, W. Yang, R. G. Parr, *Phys. Rev. B* **1988**, *37*, 785.
[19] J. P. Perdew, *Phys. Rev. B* **1986**, *33*, 8822.
[20] The starting aldehydes were obtained as follows: 1-methyl-1*H*-indole-3-carbaldehyde (**11 a**) was purchased from Sigma–Aldrich Co. Indolizine-1-carbaldehyde (**11 b**) was synthesized, in excellent yield, by a reaction sequence involving a 1,3-dipolar cycloaddition between a pyridinium *N*-methylide and an electron-deficient alkene as the key step—a) L. Zhang, F. Liang, L. Sun, Y. Hu, H. Hu, *Synthesis* **2000**, 1733. The synthesis of indolizine-3-carbaldehyde (**11 c**) was carried out by thermolysis of an allylidenedihydropyridine as previously described—b) A. Kakehi, S. Ito, T. Maeda, R. Takeda, M. Nishimura, M. Tamashima, T. Yamaguchi, *J. Org. Chem.* **1978**, *43*, 4837.
[21] B. Domínguez, R. Alvarez, A. R. de Lera, *Org. Prep. Proced. Int.* **2003**, *35*, 239.
[22] A. R. de Lera, W. Reischl, W. H. Okamura, *J. Am. Chem. Soc.* **1989**, *111*, 4051.
[23] D. Oesterhelt, *Methods Enzymol.* **1982**, *88*, 10.
[24] N. Friedman, M. Ottolenghi, M. Sheves, *Biochemistry* **2003**, *42*, 11 281.
[25] a) S. Druckmann, M. Ottolenghi, A. Pande, J. Pande, R. H. Callender, *Biochemistry* **1982**, *21*, 4953; b) M. Sheves, A. Albeck, N. Friedman, M. Ottolenghi, *Proc. Natl. Acad. Sci. USA* **1986**, *83*, 3262; c) R. Jonas, T. G. Ebrey, *Proc. Natl. Acad. Sci. USA* **1991**, *88*, 149.
[26] I. Rousso, N. Friedman, M. Sheves, M. Ottolenghi, *Biochemistry* **1995**, *34*, 12 059.
[27] M. R. Muthyala, D. Watanabe, A. E. Asato, R. S. H. Liu, *Photochem. Photobiol.* **2001**, *74*, 837.
[28] a) J. Peters, R. Peters, W. Stoeckenius, *FEBS Lett.* **1976**, *61*, 128; b) T. Schreckenbach, D. Oesterhelt, *Fed. Proc.* **1977**, *36*, 1810.
[29] D. D. Perrin, W. L. F. Armarego, *Purification of Laboratory Chemicals*, 3rd ed., Pergamon, Oxford, **1988**.

Received: April 6, 2005

